EFFECTS OF THERMAL GRADIENTS ON MEMBRANE STRESSES IN THIN SLABS

ANTHONY K. ABU[1], IAN W. BURGESS[2] and ROGER J. PLANK[3]

ABSTRACT

The Building Research Establishment (BRE) of the United Kingdom has developed a simple design method for the determination of the capacity of composite slabs in fire. The method, based on ambient temperature large-deflection plastic theory, predicts the capacity by calculating the enhancement added by tensile membrane action to the theoretical yield-line load of the slab. Tensile membrane action is a load-carrying mechanism experienced by thin slabs undergoing large vertical deflections, where stretching of the midplane produces a central area of tensile force balanced by a peripheral ring of compressive force. The use of this mechanism in structural fire engineering introduces safety and economy, as a large number of floor beams can be left unprotected. The method, developed on the assumption that the slabs are simply-supported, also assumes that the development of the tensile membrane mechanism is maintained at elevated temperatures. An analytical procedure for the determination of this membrane capacity has recently been developed by the University of Edinburgh. It argues that the development of tensile membrane action at elevated temperatures differs from that at ambient temperature, and that the tensile forces developed in the centre of the slab can only be balanced by sufficient anchorage along the slab's boundaries. Experimental investigations on large-deflection behaviour of simply-supported slabs at ambient and elevated temperatures, conducted at the University of Sheffield, have confirmed the variation in the mechanism at ambient and elevated temperatures, but have identified that the load-carrying capacity can be effectively developed without the horizontal anchorage along the slab's boundaries.

These observations have led to the belief that thermal gradients, acting alone through the depth of the slab, can induce considerable amounts of tensile membrane action. This paper therefore investigates this phenomenon in simply-supported thin slabs. It examines

[1] Research Student, Dept. of Civil & Structural Engineering, University of Sheffield, Sheffield S1 3JD, UK
Email: cip04aka@sheffield.ac.uk
[2] Professor, Dept. of Civil & Structural Engineering, University of Sheffield, Sheffield S1 3JD, UK
Email: ian.burgess@sheffield.ac.uk
[3] Professor, School of Architectural Studies, University of Sheffield, Sheffield S1 3JD, UK
Email: r.j.plank@sheffield.ac.uk

displacements and stresses developed at ambient and elevated temperatures, using the Rayleigh-Ritz approach. Good comparisons are made with finite element analyses.

1. INTRODUCTION

Real building fires and full-scale fire tests on steel-framed structures have shown that buildings possess inherent fire resistance far greater than their perceived capacities. The survival of buildings such as the uncompleted 14-storey building construction in Broadgate, London in 1990 and the Cardington fire tests of the 1990s have led to the understanding that conventional methods of protecting all steel members are very conservative[1]. In fire, if compartmentation is maintained and composite slabs are allowed to undergo large vertical deflections and two-way bending, then slabs generate a higher self-sustaining load-carrying capacity through a mechanism known as tensile membrane action. This mechanism, which increases its load capacity with increasing vertical deflection, develops as the mid-plane of the slab is stretched to produce a central area of tensile force balanced by a peripheral ring of compressive force. The effective utilisation of this capacity in structural fire engineering provides sufficient safety and economy, as a greater number of beams in a floor slab can be left unprotected [2]. Subsequent to the Cardington tests, the BRE developed a simple design method to predict the load-carrying capacity of composite slabs in fire incorporating tensile membrane action [3, 4]. The method calculates the enhancement membrane action provides in addition to the traditional flexural capacity of the slab, by considering ambient temperature conditions. Failure is based on the formation of a full-depth crack across the shorter span of the slab[3, 4]. It is assumed that the mechanism at ambient temperature is maintained at elevated temperatures[3], and an SCI design guide has been produced to facilitate the use of the method[1].

To use the BRE Membrane Action Method in the design of composite slabs in fire, a floor plate is divided into square or rectangular panels, as shown in Fig. 1. Within a panel, the

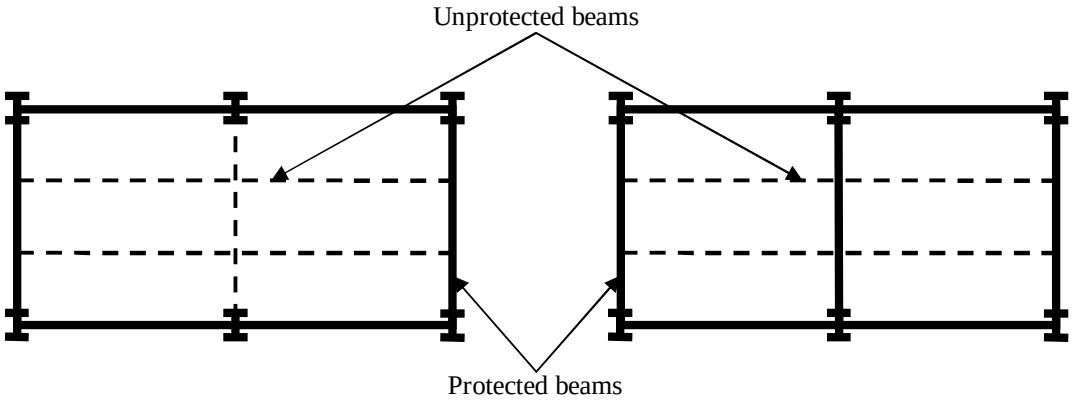

Fig. 1: Rectangular and Square Slab Panels

beams are left unprotected with protected beams on the perimeter[2]. The method, which refers to observations at Cardington, assumes that the reinforcement across the perimeter of the panel fractures, due to large hogging moments [3]. The slab panel is therefore treated as a simply supported slab on edges that resist vertical deflection. At elevated temperatures the lower layers of composite slabs are at high temperatures. Because of the low resistance of steel to heat, the contribution of the steel deck to the capacity of the concrete slab is negligible. Tests have also shown that the steel deck de-bonds from the concrete at elevated temperatures. As a result, the effective slab depth providing the necessary tensile membrane

capacity is represented as a flat slab[3], as in Fig. 2 below. In the figure, *a* is the longer span, *b* is the shorter span and *h* is the thickness.

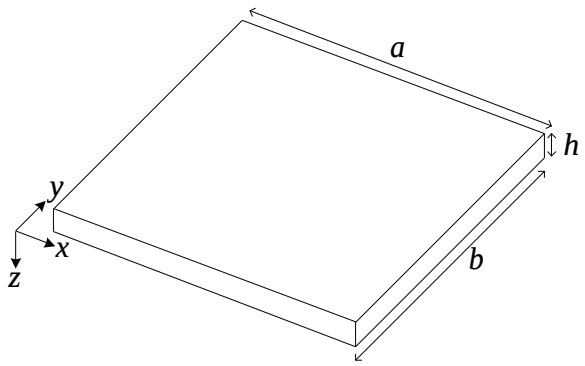

Fig. 2: Flat Slab with its dimensions

Cameron and Usmani[5, 6] have proposed a new design method to determine the membrane capacity of composite floors in fire. Their analytical method, developed from classical large-deflection theory, is a 3-step process that generates a temperature distribution through the slab; consisting of a mean temperature increase and a thermal gradient, then determines the vertical deflection and stress-strain distribution due to the thermally induced strains and, using an energy method, calculates the membrane capacity of the slab. The method assumes that the tensile forces developed in the slab can only be balanced by the provision of anchorage along the slab boundary. It assumes that this horizontal anchorage will be provided by the adjacent slabs, where an interior slab is concerned, but proposes that the design of composite beams on the edges of buildings and their connections should account for the required lateral restraint to the slabs in addition to the vertical restraint they provide.

Tests by Foster et al.[7, 8]on small-scale simply-supported flat slabs at the University of Sheffield have shown that the mode of failure of concrete slabs in fire differs from what is observed at ambient temperature. At elevated temperatures, thermal bowing of the slab induces double-curvature bending which generates full-depth cracking across the shorter span of the slab, which may lead to an eventual yield-line type of failure mechanism[7, 8]. The observations and the magnitudes of vertical deflections reached in these small-scale tests have suggested that thermal gradients acting alone through the depth of the slab can cause significant amounts of tensile membrane action in simply-supported slabs. Contrary to the suggestion by the Cameron and Usmani [5, 6], it does not seem to be necessary to provide horizontal edge restraint to sustain this load-carrying mechanism.

The research reported here, as part of a larger investigation into the analytical quantification of membrane capacity of simply-supported composite slabs in fire, looks at an initial investigation into the effects of these thermal gradients on the development of tensile membrane action and the associated stresses, using the variational Rayleigh-Ritz Method. The development of tensile membrane action at ambient and elevated temperatures is considered, and good comparisons are made with the finite element package *Vulcan*[9-10], developed over the years at the University of Sheffield.

2. LARGE DEFLECTION PLATE THEORY

Classical plate theory for medium-thick plates assumes that:

- the deflection of the mid-surface is small compared with the thickness of the plate
- the mid-plane remains unstrained subsequent to bending

- lines initially normal to the mid-surface remain normal to that surface after bending and stresses normal to the mid-plane are small compared with those in the plane of the plate and may therefore be neglected[11]

For thin plates undergoing large deflections, the first two assumptions in medium-thick plate theory are modified to account for the straining of the mid-surface, due to stretching of the plate and the contribution of the out-of-plane deflection[12]. The governing equations for large deflection theory of plates are defined as [12]:

$$\frac{\partial^4 F}{\partial x^4} + 2\frac{\partial^4 F}{\partial x^2 \partial y^2} + \frac{\partial^4 F}{\partial y^4} = E\left[\left(\frac{\partial^2 w}{\partial x \partial y}\right)^2 - \frac{\partial^2 w}{\partial x^2}\frac{\partial^2 w}{\partial y^2}\right] \tag{1}$$

$$\frac{\partial^4 w}{\partial x^4} + 2\frac{\partial^4 w}{\partial x^2 \partial y^2} + \frac{\partial^4 w}{\partial y^4} = \frac{h}{D}\left(\frac{q}{h} + \frac{\partial^2 F}{\partial y^2}\frac{\partial^2 w}{\partial x^2} + \frac{\partial^2 F}{\partial x^2}\frac{\partial^2 w}{\partial y^2} - 2\frac{\partial^2 F}{\partial x \partial y}\frac{\partial^2 w}{\partial x \partial y}\right) \tag{2}$$

F is a stress function such that:

$$N_x = h\frac{\partial^2 F}{\partial y^2}, \quad N_y = h\frac{\partial^2 F}{\partial x^2}, \quad N_{xy} = -h\frac{\partial^2 F}{\partial x \partial y} \tag{3}$$

and N_x, N_y and N_{xy} are the forces per unit length in the directions *x*, *y* and *xy*, with *w*, *q* and *D* being the vertical deflection, the load per unit area and the flexural rigidity of the plate respectively. For a plate whose origin of co-ordinates is at a corner, as in Fig. 2, exact solutions to the governing equations of large deflection theory can be obtained if the following functions are defined as[12]:

$$w = \sum_{m=1}^{\infty}\sum_{n=1}^{\infty} w_{mn} \sin\frac{mpx}{a}\sin\frac{npy}{b} \tag{4}$$

$$q = \sum_{m=1}^{\infty}\sum_{n=1}^{\infty} q_{mn} \sin\frac{mpx}{a}\sin\frac{npy}{b} \tag{5}$$

$$F = \frac{P_x y^2}{2bh} + \frac{P_y x^2}{2ah} + \sum_{m=0}^{\infty}\sum_{n=0}^{\infty} f_{mn} \cos\frac{mpx}{a}\cos\frac{npy}{b} \tag{6}$$

However, approximate solutions for the plate load-deflection behaviour are obtained if the variational Rayleigh-Ritz Method is employed[12]. The method requires that the mechanical strain energy of the plate, considering both stretching and bending, is obtained, and the amplitudes of any shape functions used in the generation of the strain and potential energies are determined by minimising the total potential energy. The coefficients determined can then be used to approximate the deflected shapes and stresses in the plate. The total strain energy and the strains at any point in the slab are given by:

$$V = \frac{E}{2(1-\nu^2)}\iiint\left[e_x^{\,2} + e_y^{\,2} + 2\nu e_x e_y + \frac{1-\nu}{2}g_{xy}^{\,2}\right]dxdydz \tag{7}$$

$$\begin{aligned} e_x &= \frac{\partial u}{\partial x} + \frac{1}{2}\left(\frac{\partial w}{\partial x}\right)^2 - z\frac{\partial^2 w}{\partial x^2}, \; e_y = \frac{\partial v}{\partial y} + \frac{1}{2}\left(\frac{\partial w}{\partial y}\right)^2 - z\frac{\partial^2 w}{\partial y^2} \\ g_{xy} &= \left(\frac{\partial u}{\partial y} + \frac{\partial v}{\partial x}\right) + \frac{\partial w}{\partial x}\frac{\partial w}{\partial y} - 2z\frac{\partial^2 w}{\partial x \partial y} \end{aligned} \tag{8}$$

To use the Rayleigh-Ritz Method functional expressions are defined for the displacements in the *x*, *y* and *z* directions, such that these expressions satisfy the geometric and natural boundary conditions. For the analyses, the origin is set in the centre of the plate (Fig. 3) and, given the symmetry of the problem, quarter-sections are modelled.

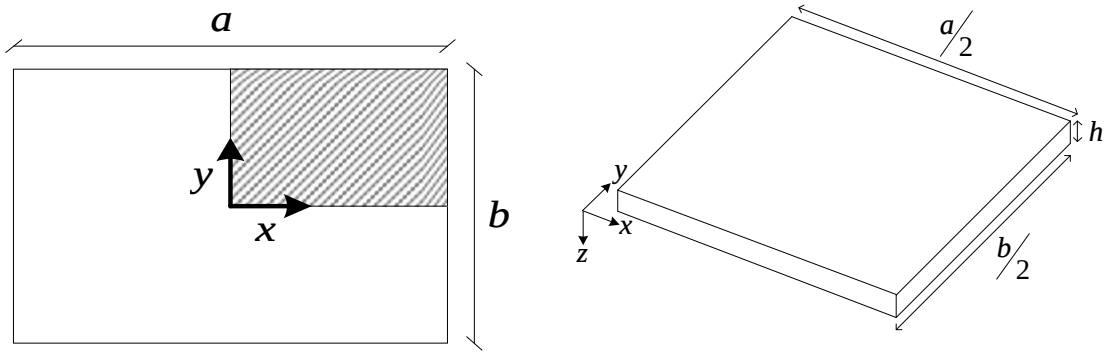

(a) Full Plate (b) Quarter Section

Fig. 3: Typical plate with its dimensions

The geometric and natural boundary conditions are:

$$N_x = 0, \quad x = \pm\frac{a}{2} \qquad M_x = 0, \quad x = \pm\frac{a}{2} \qquad N_y = 0, \quad y = \pm\frac{b}{2} \qquad M_y = 0, \quad y = \pm\frac{b}{2}$$

$$w = \frac{\partial^2 w}{\partial x^2} = \frac{\partial^2 w}{\partial y^2} = 0 \quad on\ x = \pm\frac{a}{2}\ and\ y = \pm\frac{b}{2}$$

3. SOLUTION OF THE LARGE-DEFLECTION PROBLEM

3.1 Research on Solutions of Large-Deflection Plate Problems

Attempts have been made by a number of researchers to approximate vertical deflections and stresses of thin plates under large deflections using the principle of minimum potential energy. Berger[13] proposed a strain energy equation that ignored the second invariant of the mid-surface strains. However, subsequent research established the ineffectiveness of this equation for plates with movable boundaries[14]. Banerjee and Datta[15] proposed a method that linearised the total potential energy with an expression, in terms of a factor and the vertical deflection, which gave good results if the right factor was chosen. However, there could be no physical justification for the selection of specific values for the factor. Boresi and Turner[16] proceeded by maintaining the non-linear energy equations and defining functional expressions for the in-plane strains in the *x* and *y* directions, and for the vertical deflection. Odd-numbered double Fourier series expressions were used for the strains and the vertical deflections.

3.2 Solution Adopted

For large deflection of plates, the mid-surface strains depend on the stretching of the mid-surface and the contribution of vertical deflection. Preliminary finite element analysis and observations from tests show that, for simply supported slabs subjected to large deflections, the edges (including the corners) are pulled-in. However, the expressions proposed by Boresi and Turner[16] artificially keep the corners fixed in position, preventing the slab from attaining appreciable magnitudes of displacement. The expressions are modified to

suit the observations. The in-plane strain expressions therefore require the use of the full Fourier series instead of just the odd-numbered terms. The strains are thus defined as:

$$e_x = \sum_{m=1}^{\infty}\sum_{n=1}^{\infty} A_{mn} \cos\frac{mpx}{a}\cos\frac{npy}{b}, \quad where\ m,n = 1,2,3,.... \tag{9}$$

$$e_y = \sum_{m=1}^{\infty}\sum_{n=1}^{\infty} B_{mn} \cos\frac{mpy}{b}\cos\frac{npx}{a}, \quad where\ m,n = 1,2,3,.... \tag{10}$$

with the out-of-plane deflection as:

$$w = \sum_{m=1}^{\infty}\sum_{n=1}^{\infty} W_{mn} \cos\frac{mpx}{a}\cos\frac{npy}{b}, \quad where\ m,n = 1,3,5,.... \tag{11}$$

4. AMBIENT AND ELEVATED-TEMPERATURE RAYLEIGH-RITZ ANALYSES

Tensile membrane action is deemed to have developed in a thin plate when vertical displacements are of the order of the thickness of the plate. Thus, regardless of the type of action imposed on the plate, the development of the mechanism can be observed once the magnitudes of vertical deflections are about the thickness of the plate.

The analyses were carried out on quarter-sections of horizontally unrestrained linear-elastic plates of dimensions 5000mm×5000mm×100mm. The plates had a modulus of elasticity of 18000N/mm^2 and a Poisson's ratio of 0.25. The software used for the analytical study was MAPLE 9.5 (by Waterloo Maple Inc.). Comparisons were made with the geometrically non-linear finite element analysis program *Vulcan* [9-10], but a linear-elastic material was used. For membrane tractions and stresses, results were taken at Gauss points and compared with those obtained from the analytical solution. The comparisons were made with results along 3 lines in the plate. These were along the centre-line, the edge and mid-way between these lines (see the legends in Figs. 7 and 13).

4.1 Ambient Temperature Analysis

A 100kN/m^2 (0.1N/mm^2) load was placed on the plate. The displacements and subsequent strains and stresses were determined. The horizontal displacements (u and v) in the x and y directions are given by:

$$\begin{aligned} u = {} & \frac{a}{p}\sum_{m=1}^{\infty}\sum_{n=1}^{\infty}\frac{1}{m}A_{mn}\sin\frac{mpx}{a}\cos\frac{npy}{b} \\ & -\frac{p^2}{8a^2}\sum_{m=1}^{\infty}\sum_{n=1}^{\infty} m^2 W_{mn}{}^2\left(x-\frac{a}{2mp}\sin\frac{2mpx}{a}\right)\left(1+\cos\frac{2npy}{b}\right) \end{aligned} \tag{12}$$

$$\begin{aligned} v = {} & \frac{b}{p}\sum_{m=1}^{\infty}\sum_{n=1}^{\infty}\frac{1}{n}B_{mn}\sin\frac{npy}{b}\cos\frac{mpx}{a} \\ & -\frac{p^2}{8b^2}\sum_{m=1}^{\infty}\sum_{n=1}^{\infty} n^2 W_{mn}{}^2\left(y-\frac{b}{2np}\sin\frac{2npy}{b}\right)\left(1+\cos\frac{2mpx}{a}\right) \end{aligned} \tag{13}$$

Resulting plate deflections, membrane tractions and stresses are given in Figs. 4-9. In the figures that follow, the continuous lines represent the results from the analytical model while the broken lines represent the results from the *Vulcan* finite-element analysis, as shown in

Fig. 4. A legend for each plot is given in Fig. 7 ((a) for vertical displacements, (b) for mid-plane horizontal displacements, (c) for membrane tractions and (d) for stresses).

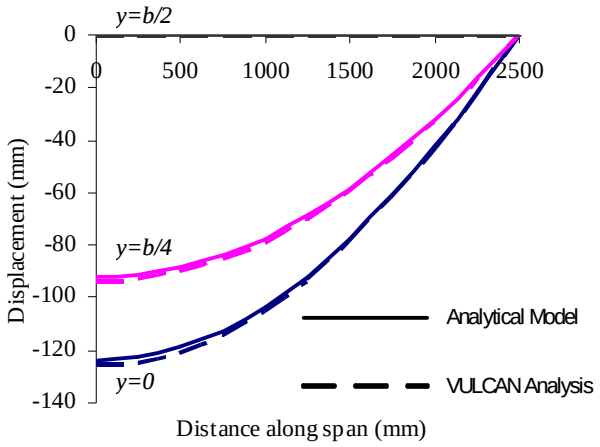

Fig 4: Ambient-temperature vertical displacements

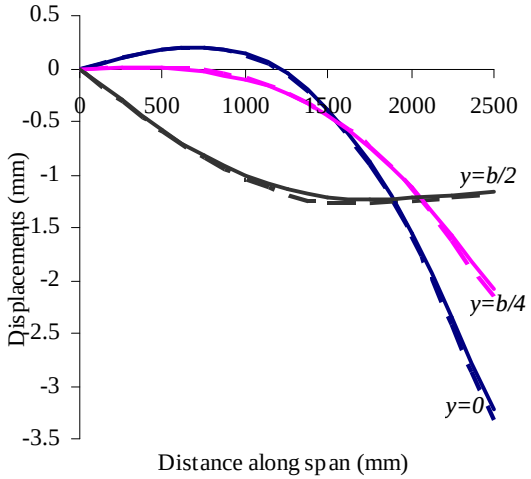

Fig 5: Ambient-temperature in-plane Displacements

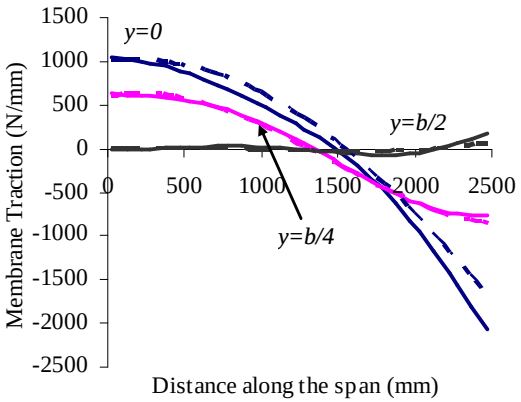

Fig 6: Ambient-temperature membrane tractions across span

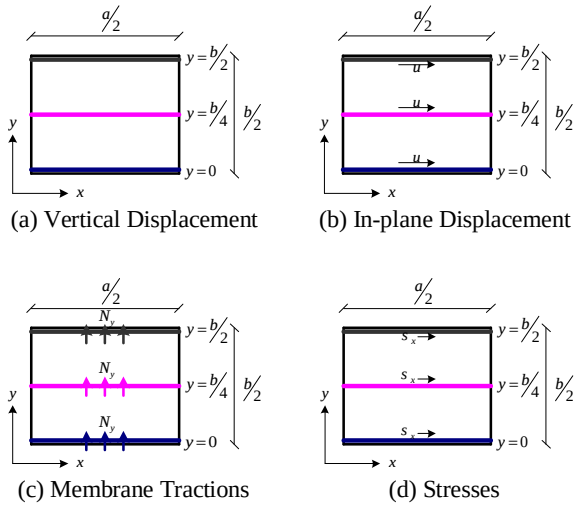

Fig 7: Ambient-temperature Legends

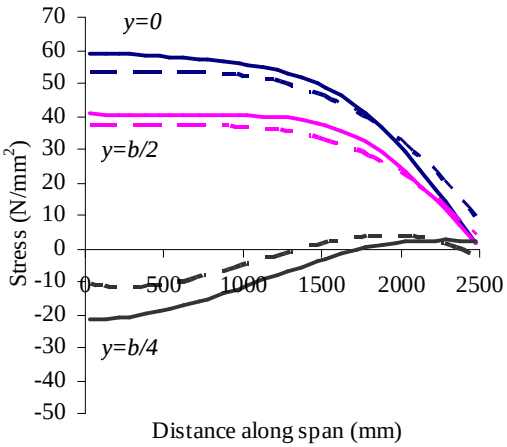

Fig 8: Ambient-temperature bottom layer stress distribution

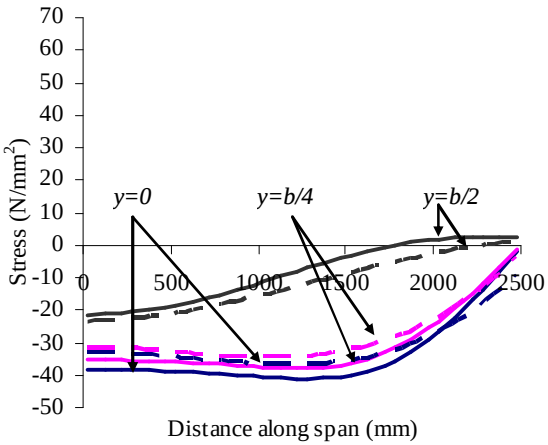

Fig 9: Ambient-temperature top layer stress distribution

4.2 Elevated Temperature Analysis

At elevated temperatures the thermal strain given by $e_t = a\Delta T$ (where α is the coefficient of thermal expansion and $\Delta T = T\text{-}T_0$ is the change in temperature at the depth being considered) influences the mechanical strains developed in the plate. For the analysis α is kept constant at $10\times10^{-6}/^{o}C$. As the aim is to investigate the effects of thermal gradients only, steady state conditions are used and a version of the *Vulcan* software which maintains room-temperature material properties is used for the comparison. The Young's modulus of the material is therefore kept at $18000N/mm^2$ in all layers, regardless of the imposed temperature gradient. No loads are imposed on the plate for the elevated-temperature analysis. The linear temperature variation between temperatures T_2 on the bottom face and T_1 on the top face is defined as[17]:

$$T = T_m + Z\frac{(T_2 - T_1)}{h}, \quad where \;\; T_m = \frac{T_1 + T_2}{2} \tag{14}$$

Therefore the mechanical strain at any point in the slab is obtained as:

$$\begin{aligned} e_x &= \frac{\partial u}{\partial x} + \frac{1}{2}\left(\frac{\partial w}{\partial x}\right)^2 - a\Delta T - z\frac{\partial^2 w}{\partial x^2}, \quad e_y = \frac{\partial v}{\partial y} + \frac{1}{2}\left(\frac{\partial w}{\partial y}\right)^2 - a\Delta T - z\frac{\partial^2 w}{\partial y^2} \\ g_{xy} &= \left(\frac{\partial u}{\partial y} + \frac{\partial v}{\partial x}\right) + \frac{\partial w}{\partial x}\frac{\partial w}{\partial y} - 2z\frac{\partial^2 w}{\partial x \partial y} \end{aligned} \tag{15}$$

The in-plane displacements thus become:

$$\begin{aligned} u = {} & \frac{a}{p}\sum_{m=1}^{\infty}\sum_{n=1}^{\infty}\frac{1}{m}A_{mn}\sin\frac{mpx}{a}\cos\frac{npy}{b} \\ & -\frac{p^2}{8a^2}\sum_{m=1}^{\infty}\sum_{n=1}^{\infty}m^2 W_{mn}{}^2\left(x - \frac{a}{2mp}\sin\frac{2mpx}{a}\right)\left(1 + \cos\frac{2npy}{b}\right) + a\Delta T x \end{aligned} \tag{16}$$

$$\begin{aligned} v = {} & \frac{b}{p}\sum_{m=1}^{\infty}\sum_{n=1}^{\infty}\frac{1}{n}B_{mn}\sin\frac{npy}{b}\cos\frac{mpx}{a} \\ & -\frac{p^2}{8b^2}\sum_{m=1}^{\infty}\sum_{n=1}^{\infty}n^2 W_{mn}{}^2\left(y - \frac{b}{2np}\sin\frac{2npy}{b}\right)\left(1 + \cos\frac{2mpx}{a}\right) + a\Delta T y \end{aligned} \tag{17}$$

Similarly, the displacements and subsequent strains and stresses can be determined. Results for plate deflections, membrane tractions and stresses are given in Figs. 10-15 for a thermal gradient of 7°C/mm. The continuous lines in the subsequent figures represent the results from the analytical model, while the broken lines represent the results from the *Vulcan* finite-element analysis, as shown in Fig. 10. Legends for the plots are given in Fig. 13 ((a) for vertical displacements, (b) for mid-plane horizontal displacements, (c) for membrane tractions and (d) for stresses).

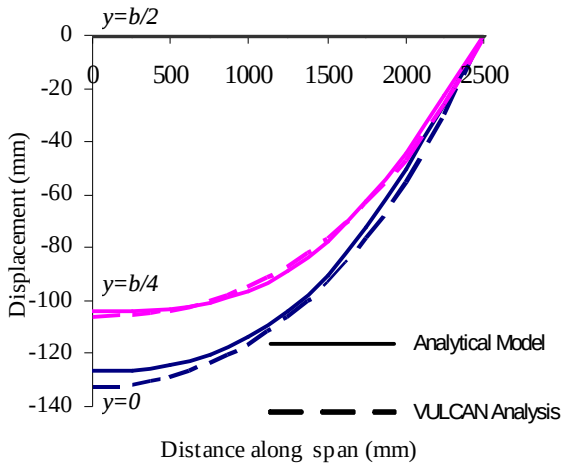

Fig 10: Elevated temperature vertical displacements

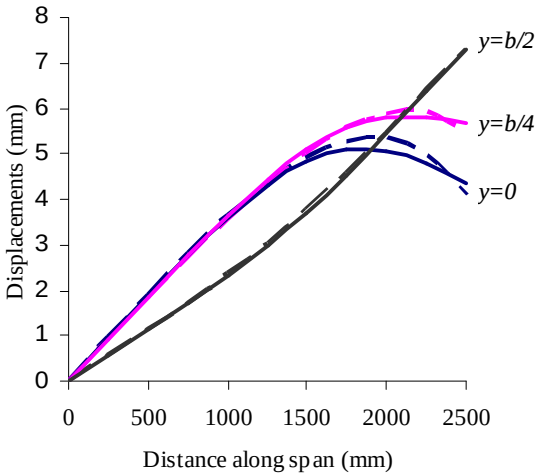

Fig 11: Elevated temperature in-plane displacements

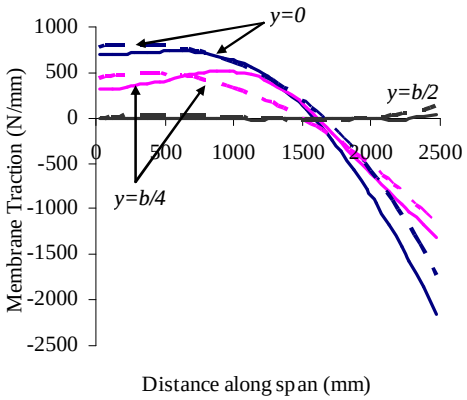

Fig 12: Elevated temperature membrane tractions across the span

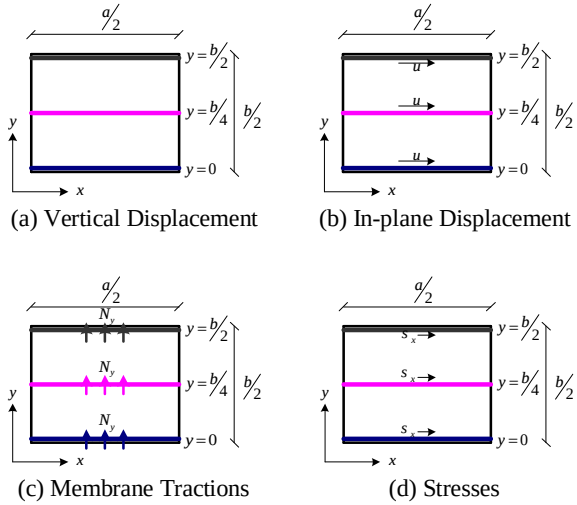

Fig 13: Elevated temperature legends

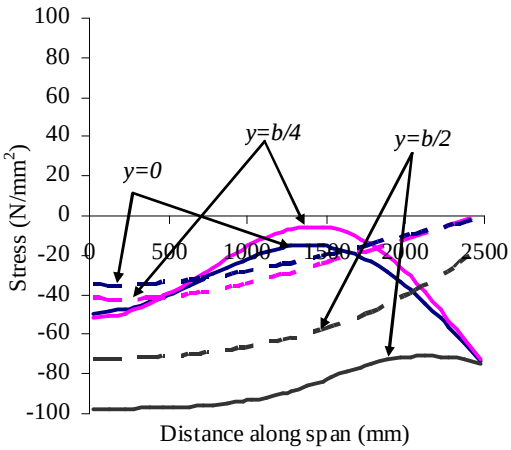

Fig 14: Elevated temperature bottom layer stress distribution

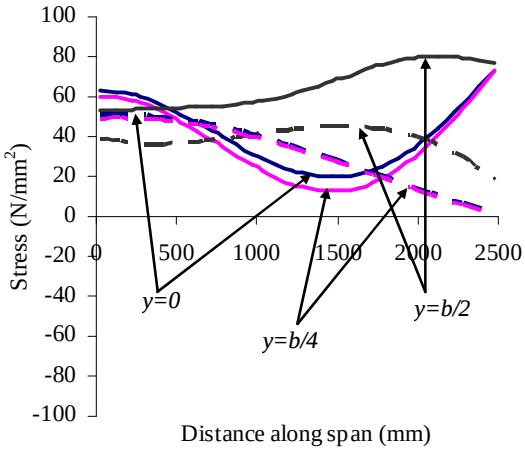

Fig 15: Elevated Temperature Top Layer Stress Distribution

5. DISCUSSIONS

The analytical solutions and the *Vulcan* results are in very good agreement. Fig.4 shows the ambient-temperature central vertical deflection as 124mm, which is greater than the thickness of the slab, confirming the tensile membrane mechanism. The horizontal displacements (Fig. 5) emphasize the existence of a tensile area with a surrounding ring of compression. The central portion of the plate is stretched, but the edges and corners are pulled-in towards the centre of the slab, creating the ring of compression. A plot of membrane forces per unit length across the span is shown in Fig. 6. Tensile forces are observed in the middle of the slab, and these decrease in magnitude and eventually become compressive forces towards the edge. Across the boundary, membrane tractions are zero in accordance with the set boundary conditions. Fig. 8 and Fig. 9 confirm the presence of tensile and compressive stresses, in the bottom and top layers respectively, of a plate loaded at ambient temperature. It also shows the compressive stresses that develop along the mid-section of the edge due to the inward movement of the edge; this stress reduces in magnitude along the edge, towards the corners.

The through-depth temperature expression used (Equation 14) combines a mean temperature increase with a thermal gradient. The thermal gradient induces vertical deflections, and as Fig. 10 shows, the central deflection from the elevated-temperature analysis (126mm) also exceeds the thickness of the plate, indicating the presence of tensile membrane action. A uniform thermal expansion would have produced horizontal displacements of 8.75mm along the edge of the plate, but stretching of the mid-regions of the plate and the corresponding inward movement of the edges and corners generate the displacements shown in Fig. 11. In similar fashion to the ambient-temperature case, membrane tractions are plotted in Fig. 12. These also show the presence of tensile forces in the centre of the plate with compressive forces along the periphery. When an unloaded slab is exposed to heat on its bottom surface, thermal expansion of hotter lower layers against cooler upper layers creates compressive stresses in the lower layers and tensile stresses in the upper layers (Fig. 14 and Fig. 15).

For the central region of the plate, where tensile membrane forces are present, the method gives a good prediction of the stresses, but fails to do so for the area where in-plane stresses are controlled by the presence of the compressive ring. An investigation into this behaviour, conducted on uniformly heated plates, revealed that, due to the limitations of the Rayleigh-Ritz approach, complete convergence was only attainable with excessively high numbers of strain and vertical displacement expressions. An automatic solution procedure has proved very difficult to implement, as the procedure could not be transformed into a numerical process.

6. CONCLUSION

The method has shown that differential thermal expansion through the depth of a simply-supported slab can induce a considerable amount of tensile membrane action. It has also proved that it is not necessary to design edge beams and their connections to provide lateral restraint as the compressive ring develops, irrespective of the horizontal restraint along the boundary. The next step in the project is to investigate the influence of these thermal gradients and restraints along the boundary on the development of membrane action. It is hoped that this research will help establish the true mechanism of tensile membrane action in composite slabs at high temperatures, so that the necessary steps can be taken to harness this self-sustaining load-carrying mechanism.

REFERENCES

[1] Newman, G. M., Robinson, J. T., Bailey, C. G. "Fire Safe Design: A New Approach to Multi-Storey Steel-Framed Buildings." SCI Publication P288 (2000)

[2] Bailey C. G. "Membrane of slab/beam composite floor systems in fire". Engineering Structures **26** (2004), pp1691-1703

[3] Bailey C. G. "Design of Steel Structures with Composite Slabs at the Fire Limit State. Final Report prepared for the Department of the Environment, Transport and the Regions, and the Steel Construction Institute, Report No. 81415." The Building Research Establishment (2000)

[4] Bailey C. G. "Membrane action of unrestrained lightly reinforced concrete slabs at large displacements." Engineering Structures **23** (2001), pp470-483

[5] Cameron N. J. K., Usmani A. S., "New design method to determine the membrane capacity of laterally restrained composite floor slabs in fire. Part 1: Theory and method." The Structural Engineer **83** (2005), pp28-33

[6] Cameron N. J. K., Usmani A. S., "New design method to determine the membrane capacity of laterally restrained composite floor slabs in fire. Part 2: Validation." The Structural Engineer **83** (2005), pp34-39

[7] Foster S. J., Bailey C. G., Burgess I. W., Plank R. J. "Experimental behaviour of concrete floor slabs at large displacements." Engineering Structures **26** (2004), pp1231-1247

[8] Foster S. J., Burgess I. W., Plank R. J. "Investigation of Membrane Action in Model scale slabs subjected to high temperatures." Proceedings of the 4th International conference of Advances in Steel Structures, Vol. II, Shanghai, China (2005), pp933-940

[9] Huang Z., Burgess I. W., Plank R. J. "Modelling Membrane Action of Concrete Slabs in Composite Buildings in Fire. I: Theoretical Development." ASCE Journal of Structural Engineering **129** (8) (2003), pp1093-1102

[10] Huang Z., Burgess I. W., Plank R. J. "Modelling Membrane Action of Concrete Slabs in Composite Buildings in Fire. II: Validations." ASCE Journal of Structural Engineering **129** (8) (2003), pp1103-1112

[11] Park, R. and Gamble, W. L. "Reinforced Concrete Slabs." Second Edition, John Wiley and Sons Ltd. (2000)

[12] Timoshenko, S. and Woinowsky-Krieger S. "Theory of Plates and Shells." International Student Edition, Second Edition, McGraw-Hill Book Company, Inc. (1959)

[13] Berger, H. M. "A New Approach to the Analysis of Large Deflections of Plates." Journal of Applied Mechanics, Volume **22** (1955), pp465-472

[14] Nowinski, J. L. and Ohnabe, H. "On certain inconsistencies in Berger equations for large deflections of elastic plates." International Journal of Mechanical Sciences, volume **14** (1958), pp165

[15] Banerjee, B. and Datta, S. "A new approach to an analysis of large deflections of thin elastic plates." International Journal of Non Linear Mechanics, volume **16** No. 1 (1981), pp47-52

[16] Boresi, A. P. and Turner, J. P. "Large Deflections of Rectangular Plates." International Journal of Non Linear Mechanics, volume 18 No. **2** (1983), pp125-131

[17] Johns, D. J. "Thermal Stress Analyses." Pergamon Press Ltd. (1965)